THE ENVIRONMENT-DEPENDENT INTERATOMIC POTENTIAL APPLIED TO SILICON DISORDERED STRUCTURES AND PHASE TRANSITIONS

MARTIN Z. BAZANT*, EFTHIMIOS KAXIRAS* and J. F. JUSTO**
*Department of Physics, Harvard University, Cambridge, MA 02138, bazant@cmt.harvard.edu
**Instituto de Fisica da Universidade de São Paulo, CP 66318, CEP 05315-970 São Paulo - SP, Brazil

ABSTRACT

The recently developed Environment-Dependent Interatomic Potential (EDIP) holds the promise of a new degree of transferability in describing bulk phases and defects of elemental covalent solids with a simple theoretically motivated functional form. Here we explore to what extent the environment-dependence of the model can extrapolate successes of the fitted version for Si for bulk defects to disordered phases, which involve local configurations very different from those used in fitting. We find that EDIP-Si provides an improved description of the metallic bond angles of the liquid and is the first empirical potential to predict a quench directly from the liquid to the amorphous phase. The resulting amorphous structure is in closer agreement with *ab initio* and experimental results than with any artificial prepration method. We also show that melting of the bulk crystal and premelting of the (100)2×1 surface are reasonably well described by EDIP-Si in spite of its not being fit to any such properties.

INTRODUCTION

The availability of realistic and efficient interatomic potentials could have a major impact on the microscopic understanding of materials properties, for two basic reasons. The first is that simulations would be possible of complex processes requiring too many atoms or too long times to be feasible for simulation with a quantum-mechanical treatment of the electrons. The second benefit offered by a realistic interatomic potential is a conceptual framework in which to understand the complexities of chemical bonding. For example, the natural partitioning of total energy among the atoms and the distinction between radial and angular forces are very useful concepts for building intuition about atomic behavior in materials.

The difficulty in exploiting these benefits is that they are accompanied by serious drawbacks. The first is that there is no general and systematic method for deriving interatomic potentials that has demonstrated superiority over the ubiquitous "guess-and-fit" approach, which is to guess a functional form containing adjustable parameters and then to fit them to some set of experimental or *ab initio* data. Secondly, once one has an interatomic potential, its transferability is often in doubt. In other words, the potential cannot reliably describe structures different from those used in the fitting.

These problems have been most serious for covalently bonded solids, as exemplified by the prototypical case of silicon for which there are over 30 potentials in the literature, having a wide range of functional forms and fitting strategies but possessing comparable overall accuracy [1]. In spite of intense recent efforts, the simple, pioneering potentials of Stillinger-Weber (SW) and Tersoff continue to be the most popoular, albeit with well-documented limitations [1]. This experience suggests that the most successful approach is to build the essential physics into a simple functional form containing only a few adjustable parameters rather than brute-force fitting. The latter method, in our view also undermines the benefits of potentials described above: an overly complex functional form at the same time reduces the efficiency of force computation and hinders physical interpretation.

THE ENVIRONMENT-DEPENDENT INTERATOMIC POTENTIAL

In an effort to go beyond the practical limits of the guess-and-fit approach, we have provided *ab initio* theoretical guidance to motivate a functional form for interactions in covalent solids, which we call the Environment-Dependent Interatomic Potential (EDIP) [2]. Exact inversions of *ab initio* cohesive energy curves for silicon reveal global trends in bonding from covalent to metallic structures [3], and an analysis of elastic properties of the diamond and graphitic structures quantifies the mechanical properties of sp^2 and sp^3 hybrid covalent bonds [2]. We argue that the fundamental limitation of existing potentials is their inability to properly adapt bonding preferences to the local atomic environment, which is crucial for reproducing phase transitions.

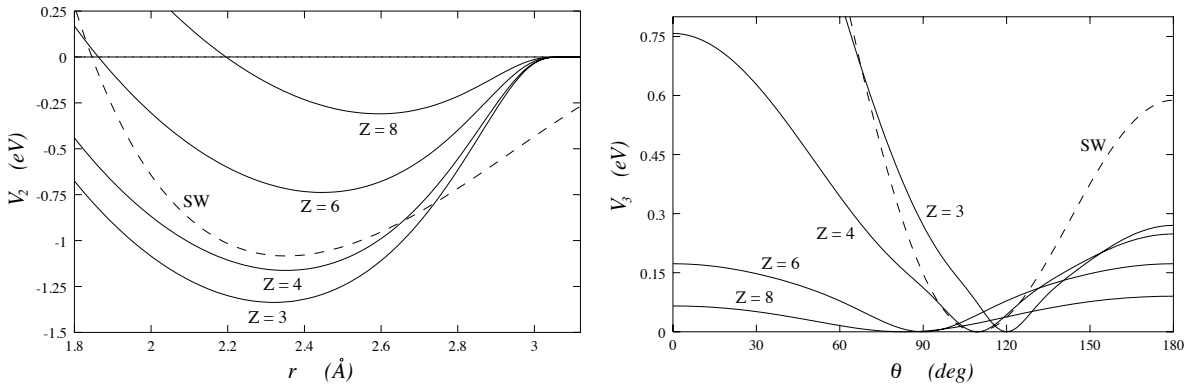

Figure 1: (Left) EDIP-Si two-body interaction $V_2(r, Z)$ as a function of separation r shown for coordinations 3, 4, 6 and 8. (Right) EDIP three-body interaction $V_3(r, r, \cos\theta, Z)$ for a pair of bonds of fixed length $r = 2.35$ Å subtending an angle θ, shown for coordinations 3, 4, 6 and 8. Each interaction is compared with the corresponding *environment-independent* term in the SW potential.

We now present the EDIP functional form and refer the reader to Ref. [2] for theoretical justification of all the terms. The energy of a configuration $\{\vec{R}_i\}$ is expressed as a sum over single-atom energies, $E = \sum_i E_i$, each containing radial and angular terms,

$$E_i = \sum_{j \neq i} V_2(R_{ij}, Z_i) + \sum_{j \neq i} \sum_{k \neq i, k > j} V_3(\vec{R}_{ij}, \vec{R}_{ik}, Z_i), \tag{1}$$

each dependent on the local atomic environment through an effective coordination number, $Z_i = \sum_{m \neq i} f(R_{im})$, where $f(r)$ is a cutoff function that determines the contribution to an atom's coordination from each of its neighbors,

$$f(r) = \begin{cases} 1 & \text{if } r < c \\ \exp\left(\frac{\alpha}{1-x^{-3}}\right) & \text{if } c < r < a \\ 0 & \text{if } r > a \end{cases} \tag{2}$$

where $x = \frac{(r-c)}{(a-c)}$. The environment-dependent radial term takes the form of a (second moment) bond order model similar to embedded-atom potentials for metals,

$$V_2(r, Z) = A \left[\left(\frac{B}{r}\right)^{\rho} - \mathrm{e}^{-\beta Z^2} \right] \exp\left(\frac{\sigma}{r-a}\right). \tag{3}$$

The strength of the attraction varies with coordination as dictated by inversion of cohesive energy curves [3]: as shown in Fig. 1, bond lengths get weaker and longer with increasing coordination, modeling sp^2 and sp^3 hybrid bonds and the covalent to metallic transition. The angular term essential for covalent bonding,

$$V_3(r, r', \theta, Z) = \lambda \exp\left(\frac{\gamma}{r-a}\right) \exp\left(\frac{\gamma}{r'-a}\right) H\left((\cos\theta + \tau(Z)) Q_\circ^{1/2} e^{-\mu Z/2}\right), \tag{4}$$

$$H(x) = 1 - \mathrm{e}^{-x^2} + \eta x^2, \tag{5}$$

also contains strong adaptation to the local environment through the the preferred angle $\cos^{-1}\tau(Z)$ and the variable strength of the angular function $e^{-\mu Z/2}$. The function $\tau(Z)$ is chosen (before fitting the potential) to interpolate between values suggested by theory ($\tau(4) = 1/3$, $\tau(3) = 1/2$, $\tau(6) = \tau(2) = 0$),

$$\tau(Z) = u_1 + u_2(u_3 e^{-u_4 Z} - e^{-2u_4 Z}), \tag{6}$$

with the parameters $u_1 = -0.165799$, $u_2 = 32.557$, $u_3 = 0.286198$, and $u_4 = 0.66$. As shown in Fig. 1, the angular function shifts its preferred angle to mimick covalent rehybridization for $Z \leq 4$ and softens considerably for overcoordinated, metallic environments.

Recently, we have presented a version of EDIP with 13 parameters fitted for bulk defects in silicon that displays remarkable transferability for bulk properties (elastic constants, bulk crystal structures, point

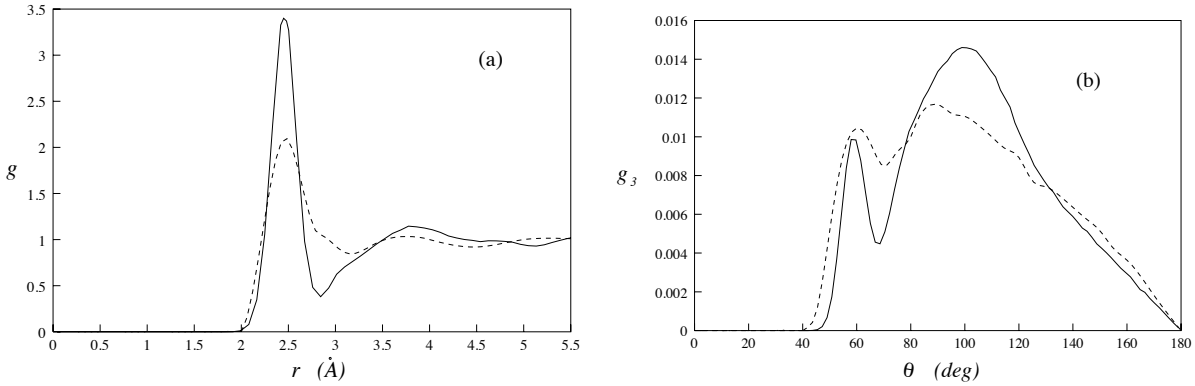

Figure 2: (Left) pair correlation function and (right) bond angle distribution for the liquid at $T = 1800$ K and $P = 0$ with EDIP-Si (solid lines) and an *ab initio* model [5] (dashed lines).

defects, concerted excahnge, stacking faults and dislocation core properties) [4]. The optimal parameter set we found is: $A = 7.9821730$ eV, $B = 1.5075463$, $\rho = 1.2085196$, $a = 3.1213820$ Å, $c = 2.5609104$ Å, $\sigma = 0.5774108$ Å, $\lambda = 1.4533108$ eV, $\gamma = 1.1247945$ Å, $\eta = 0.2523244$, $Q_\circ = 312.1341346$, $\mu = 0.6966326$, $\beta = 0.0070975$ and $\alpha = 3.1083847$. Since the fitted cutoff distance 3.1213820 Å is smaller than the SW cutoff, computing forces with our model is typically faster than with the SW potential (using an efficient algorithm [2]), making it possible to simulate thousands of atoms for millions of time steps in one day on typical workstation. Of course, at the moment this kind of efficiency is well beyond the reach of more accurate quantum-mechanical methods.

LIQUID PHASE

With the ability to simulate large systems for long times, it is natural to turn our attention to disordered structures and phases transitions. These situations contain a rich set of local bonding states from covalent (amorphous) to metallic (liquid) about which no information was included in our fitting procedure, thus constituting a stringent test of transferability for the model. Existing potentials have had considerable difficulty in simultaneously describing the crystalline, liquid and amorphous phases [1, 5, 6, 9]. In the case of the liquid, environment-independent potentials are not able to reproduce the bond angle distribution of the liquid[9], which deviates significantly from the tetrahedral angle.

We prepared a 1728-atom liquid sample with EDIP-Si potential at $T = 1800$ K and zero pressure in two ways, using standard techniques (Anderson piston, velocity rescaling, 5th order Gear predictor corrector integration). First, following a lattice start at 4000 K, the sample is cooled and equilibrated for about 50 ps. The same structure is also produced by heating a periodic bulk crystal, but the solid superheats before melting (an issue we address below). The latent heat of melting is 37.8 kJ/mol, in reasonable agrement with the experimental value of 50.7 kJ/mol, closer than the SW value of 31.4 kJ/mol [10]. The structural properties of the EDIP-Si liquid are shown in Fig. 2 and compared with the results of 64-atom *ab initio* simulations[5]. From the area under the first peak of $g(r)$, the coordination of the EDIP-Si liquid is 4.5, well below the experimental value of 6.5. Although this is unphysical, EDIP-Si offers a qualitative improvement in the bond angle distribution function $g_3(\theta, r_m)$. As shown in Fig. 2, EDIP-Si reproduces the auxiliary maximum at $\theta = 60°$, and is the first to do so, although the primary maximum is shifted toward the tetrahedral angle away from the *ab initio* most probable angle of $\theta = 90°$. It is important to emphasize that reasonable liquid properties are predicted by our model without any explicit fitting to the liquid phase. The reduced density and excess of covalent bonds may be artifacts of the short cutoff of our potential, which is appropriate for the covalently-bonded structures used in the fitting, but is perhaps too short to reproduce overcoordination in metallic phases like the liquid.

AMORPHOUS PHASE

Experimentally, amorphous silicon is known to form a random tetrahedral network, with long-range disorder and short-range order similar to that of the crystal [7, 8]. *Ab initio* simulations with 64 atoms

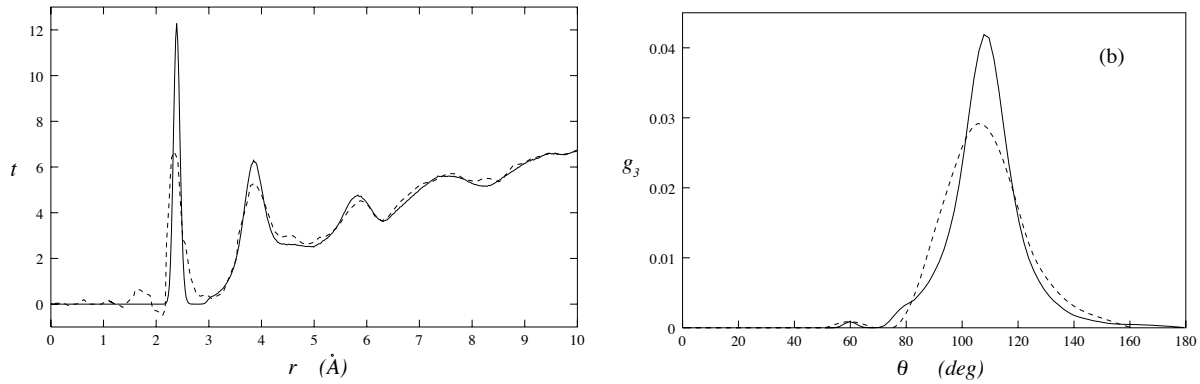

Figure 3: (Left) radial distribution function $t(r) = 4\pi\rho r g(r)$ for the amorphous phase at $T = 300$ K and $P = 0$ predicted by EDIP-Si (solid line) compared with the results of neutron scattering experiments[7]. (Right) bond angle distribution for EDIP-Si compared with *ab initio* results[6] (dashed lines).

	ρ_a	ΔH_{a-c}	$\overline{Z}$	$\overline{r}_1$	σ_{r_1}	$\overline{r}_2$	$\overline{r}_3$	$\overline{\theta}$	σ_θ
EDIP	0.04836	0.22	4.054	2.39	0.034	3.84	5.83	108.6	14.0
EXPT	0.044–0.054	< 0.19	3.90–3.97	2.34–2.36	0.07–0.11	3.84	5.86	108.6	9.4–11.0
LDA	-	0.28	4.03	2.38	0.079	3.84	-	108.3	15.5

Table I: Comparison of thermodynamic and structural properties of the present model (EDIP) for a-Si with (annealed) *ab initio*[6] and with (annealed) experimental[6, 7, 8] results. Shown are the density ρ_a in Å^{-3}, the excess enthalpy ΔH_{a-c} compared to the crystal in eV/atom, the coordination $\overline{Z}$, the mean $\overline{r}_1$ and deviation σ_{r_1} of the first neighbor distance in Å, the mean second $\overline{r}_2$ and third $\overline{r}_3$ neighbor distances in Å and the mean $\overline{\theta}$ and deviation σ_θ of the bond angles in degrees.

find almost 97% four-fold coordination [6]. An empirical potential would be invaluable in exploring larger system sizes and longer relaxation times than are feasible from first principles, but unfortunately no existing potential is capable of quenching directly from the liquid to the amorphous phase. Instead, empirical model liquids (like SW) typically transform into glassy phases upon cooling, characterized by frozen-in liquid structure [10]. Therefore, it has been impossible to simulate an experimentally relevant path to the amorphous structure (*e.g.* laser quenching [8]), and artificial preparation methods have been required to create large-scale amorphous structures [10, 11], but these do not involve realistic dynamics.

Remarkably, the EDIP-Si predicts a quench directly from the liquid into a high-quality amorphous structure. The phase transition is quite robust, since it occurs even with fast cooling rates. For example, quenching at -300 K/ps leads to a reasonable structure with 84% four-fold coordination. At much slower quench rates of -1 K/ps, an improved structure of 1728 atoms at $T = 300$ K and zero pressure is produced with almost 95% four-fold coordination. For comparison, the most common artificial prepration methods do not perform so well: the indirect SW method [10] predicts 81% four-fold coordination and the bond-switching algorimth of Wooten-Winer-Weaire [11] predicts 87%.

As shown in Fig. 3, the radial distribution function $t(r) = 4\pi\rho r g(r)$ is in excellent agreement with the results of neutron scattering experiments by Kugler *et. al.* [7] (using their experimental density $\rho = 0.054$ atoms/Å^3 for comparison). The persistence of intermediate-range order up to 10 Å captured by our model as in experiment is a strength of the empirical approach, since this distance is roughly the size of the periodic simulation box used in the *ab initio* studies [6]. Given the limited resolution of the experimental data, especially at small r (large q in the structure factor), the sharper first three peaks with our model may be interpreted as refinements of the experimental results. The bond angle distribution $g_3(\theta, r_m)$ shown in Fig. 3 (b) is narrowly peaked just below the tetrahedral angle, and also reproduces the small, well-separated peak at 60° observed in *ab initio* simulations [6] (unlike in previous empirical models). The peaks in both $g(r)$ and $g_3(\theta, r_m)$ are narrower and taller with EDIP-Si than with *ab initio* methods, which probably reflects the small system size and short times of the *ab initio* simulations compared to ours.

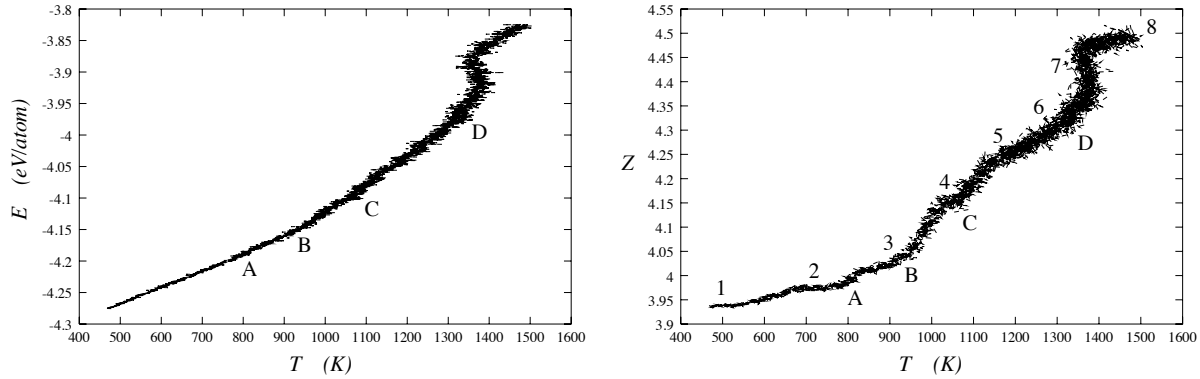

Figure 4: (Left) total energy and (right) average EDIP coordination number for a simulation of melting of a 3405-atom crystallite with (100)2×1 surfaces using EDIP-Si.

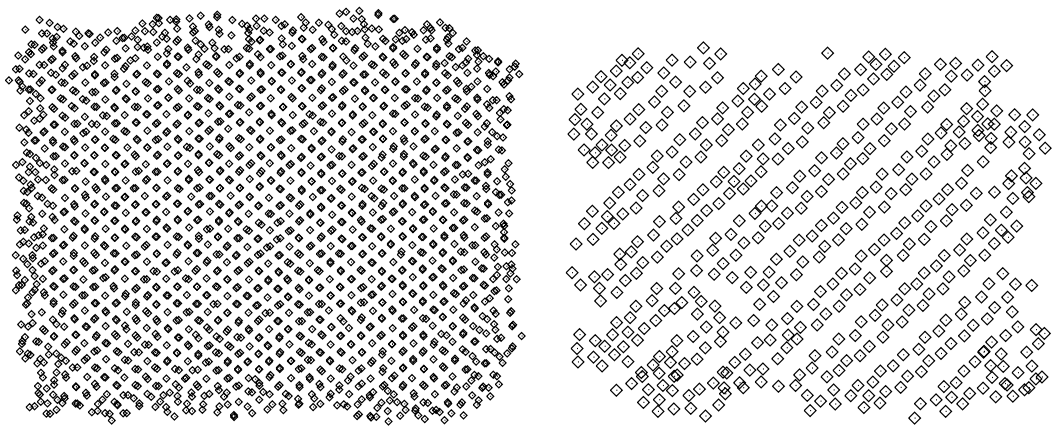

Figure 5: Two slices (12 Å thick) of the melting sample taken at stage 4, $T = 1000$ K. (Left) premelting of narrow (100) ledges. (Right) one of the two 7 nm × 7nm (100)2×1 surface just prior to the onset of premelting showing the presence of surface defects.

In Table I we summarize a detailed comparison of features of a-Si as obtained with our model and with ab-initio methods, against those revealed by experiment. Overall the agreement with experiment is very satisfactory, with the results of the present model somewhat closer to experimental values than ab-initio results as in the case of the enthalpy and the bond-length and bond-angle deviations. In summary, EDIP-Si faithfully reproduces the structure of amorphous silicon, following a realistic preparation procedure that starts with a liquid phase and cools it down without any artificial changes.

BULK MELTING AND SURFACE PREMELTING

Simulations of bulk melting with periodic boundary conditions have trouble in pinning down the melting point, as indicated by the spread of values reported for SW [1]. The problem is that in a periodic, defect-free crystal it is difficult for the system to nucleate the liquid phase. This difficulty is removed by introducing surfaces, which also allows us to study surface premelting. We performed simulations of 3405 crystal atoms arranged in a finite slab (7 nm × 7nm × 1.5 nm) terminated by (100)2×1 surfaces. The dimer reconstruction was artificially imposed on the original sample to avoid waiting for dimer rows to form spontaneously.

The sample was gradually melted by adding heat at a constant rate (by rescaling velocities) from 300 K to 1500 K in 2 ns (over 10 million time steps). Although a bulk periodic solid superheats and melts at around 2200 K, the finite slab undergoes a sharp, first-order transition at 1370 ± 20 K, as shown in Fig. 4. This is 20% below the experimental value of 1685 K, which is the closest agreement with the

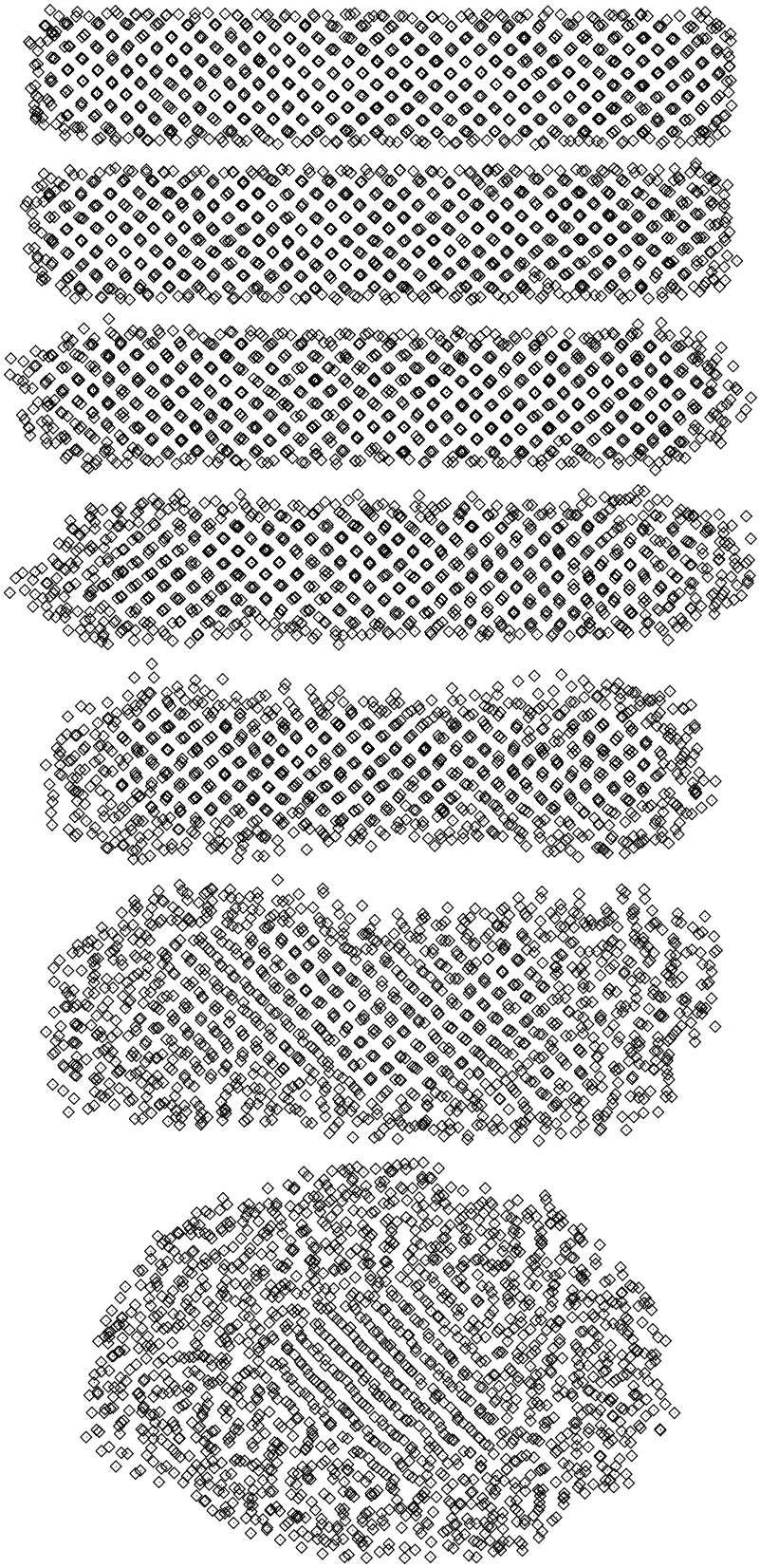

Figure 6: Snapshots taken at 0.2 ns (one million step) intervals of a simulation of a 3405-atom crystallite melting using EDIP-Si. The seven images from top to bottom correspond to the states 1–7 labeled in Fig. 4(b). The eighth state (not shown) is a spherical liquid drop.

melting point reported for any potential that was not explicitly fit to reproduce it[1]. The energy versus temperature curve shows some structure below the bulk melting point, but changes are much more clearly seen in the average EDIP coordination number, a convenient measure of local order. The system passes through 8 distinct states labeled in Fig. 4 and displayed in Fig. 6: (1) well-equilibrated (100)2×1 surfaces; (2) reconstructed edges exposing narrow (110) facets, give the sample a "beveled" look; (3) after passing through point A at 810 K, the edges and corners premelt, leaving faces intact; (4) after passing through point B at 950 K the narrow (2-4 dimers wide) (100)2×1 surfaces premelt, but the large surfaces do not. At this time, the large surfaces have some defects and mobile adatoms, as shown in Fig. 5; (5) after passing though point C at 1080 K, the large surfaces melt leaving two premelted monolayers encasing sample; (6) as the bulk melting point is approached, more layers premelt and surface and interface tension drive the sample to be more spherical by surface flow. The anisotropy of interfacial tension drives the interior crystallite to form (110) and (111) facets; (7) at $T = 1370$ K, added energy converts the bulk solid into liquid, leaving (8) a spherical liquid drop. Although the details of this simulation, primarily surface dynamics need to be more carefully validated, it demonstrates that EDIP-Si predicts premelting of the (100)2×1 surface about 300 K below the bulk melting point, consistent with experiment. Given our extensive tests for the liquid, amorphous and bulk defects, we may expect that the dynamics of the liquid-solid interface are fairly realistic by the usual standards.

CONCLUSION

In conclusion, EDIP-Si provides an improved description of disordered bulk structures and phase transitions. It is the first potential to predict the quench from liquid to amorphous and the structure is in excellent agreement with experimental and *ab initio* results. It also appears to describe several aspects of surface premelting, and predicts the bulk melting point to within 20%. These new results taken together with known successes for bulk defects suggest that EDIP-Si may be useful in applications such as solid and liquid phase epitaxial growth or radiation damage. Finally, we remark that the theoretical analysis which guided the development of EDIP-Si may be useful in extending the model to related covalent materials (Ge, C and possibly alloys).

ACKNOWLDGMENTS

Partial support was provided to MZB by the Harvard MRSEC , which is funded by NSF grant number DMR-94-00396 and to JFJ by the Brazilian Agency CNPq. MZB acknowldges useful discussions with Noam Bernstein.

REFERENCES

1. For a recent review, see H. Balamane, T. Halicioglu, and W. A. Tiller, Phys. Rev. B **46**, 2250 (1992).
2. M. Z. Bazant, E. Kaxiras and J. F. Justo, Phys. Rev. B **56**, 8542 (1997).
3. M. Z. Bazant and E. Kaxiras, Phys. Rev. Lett. **77**, 4370 (1996).
4. J. F. Justo, M. Z. Bazant, E. Kaxiras, V. V. Bulatov and S. Yip, submitted to Phys. Rev. B (1997).
5. I. Štich, R. Car and M. Parinello, Phys. Rev. B **44**, 4262 (1991); Phys. Rev. Lett. **63**, 2240 (1989).
6. I. Štich, R. Car, and M. Parrinello, Phys. Rev. B **44**, 11092 (1991).
7. S. Kugler, G. Molinar, G. Petö, E. Zsoldos, L. Rosta, A. Menelle and R. Bellissent, Phys. Rev. B **40**, 8030 (1989).
8. J. Fortner and J. S. Lannin, Phys. Rev. B **39**, 5527 (1989); Roorda, W. C. Sinke, J. M. Poate, D. C. Jacobson, S. Dierker, B. S. Dennis, D. J. Eaglesham, F. Spaepen and P. Fuoss, Phys. Rev. B **44**, 3702 (1991).
9. M. Ishimaru, K. Yoshida, and T. Motooka, Phys. Rev. B **53**, 7176 (1996).
10. J. Q. Broughton and X. P. Li, Phys. Rev. B **35**, 9120 (1987); W. D. Luedtke and U. Landman, Phys. Rev. B **37**, 4656 (1988).
11. F. Wooten, K. Winer and D. Weaire, Phys. Rev. Lett. **54**, 1392 (1985).